Title

Cytoglobin deficiency potentiates Crb1-mediated retinal degeneration in rd8 mice

Journal

Developmental Biology, 458(2)

ISSN

0012-1606

Authors

Kwon, Young Sam
Tham, Addy
Lopez, Antonio Jacobo
et al.

Publication Date

2020-02-01

DOI

10.1016/j.ydbio.2019.10.013

Peer reviewed

HHS Public Access

Author manuscript

Dev Biol. Author manuscript; available in PMC 2021 February 15.

Published in final edited form as:

Dev Biol. 2020 February 15; 458(2): 141–152. doi:10.1016/j.ydbio.2019.10.013.

Cytoglobin deficiency potentiates *Crb1*-mediated retinal degeneration in *rd8* mice

Young Sam Kwon, DVM PhD[1,2], **Addy Tham**[1], **Antonio Jacobo Lopez**[1], **Sydney Edwards, D.V.M.**[3], **Sean Woods**[1], **Jiajia Chen, M.D.**[1], **Jenna Fortunato**[1], **Alejandra Quiroz**[1], **Seanne Javier**[1], **Ingrid Au**[1], **Maria Clarke**[1], **Devin Humpal**[1], **K. C. Kent Lloyd, D.V.M. Ph.D.**[4,5], **Sara Thomasy, D.V.M. Ph.D.**[1,3], **Christopher Murphy, D.V.M. Ph.D.**[1,3], **Thomas M. Glaser, M.D. Ph.D.**[6], **Ala Moshiri, M.D. Ph.D.**[1,§]

[1.]Department of Ophthalmology and Vision Science, School of Medicine, U.C. Davis, Sacramento, CA, United States

[2.]College of Veterinary Medicine, Kyungpook National University, Daegu, South Korea

[3.]Department of Surgical and Radiological Sciences, School of Veterinary Medicine, U.C. Davis, Davis, CA, United States

[4.]Mouse Biology Program, U.C. Davis, Davis, CA, United States

[5.]Department of Surgery, School of Medicine, U.C. Davis, Sacramento, CA, United States

[6.]Department of Cell Biology and Human Anatomy, School of Medicine, U.C. Davis, Davis, CA, United States

Abstract

Purpose: The purpose of this study is to determine the effect of Cytoglobin (Cygb) deficiency on Crb1-related retinopathy. The Crb1 cell polarity complex is required for photoreceptor function and survival. Crb1-related retinopathies encompass a broad range of phenotypes which are not completely explained by the variability of Crb1 mutations. Genes thought to modify Crb1 function are therefore important targets of research. The biological function of Cygb involves oxygen delivery, scavenging of reactive oxygen species, and nitric oxide metabolism. However, the relationship of Cygb to diseases involving the Crb1 cell polarity complex is unknown.

Methods: Cygb knockout mice homozygous for the rd8 mutation ($Cygb^{-/-rd8/rd8}$) were screened for ocular abnormalities and imaged using optical coherence tomography and fundus photography. Electroretinography was performed, as was histology and immunohistochemistry. Quantitative PCR was used to determine the effect of Cygb deficiency on transcription of Crb1 related cell polarity genes.

[§]Corresponding author: Ala Moshiri MD PhD, U.C. Davis Eye Center, 4860 Y Street, Suite 2400, Sacramento, California, 95817, Phone: (916) 734-6074, Fax: (916) 734-6992, amoshiri@ucdavis.edu.

Results: Cygb$^{-/-rd8/rd8}$ mice develop an abnormal retina with severe lamination abnormalities. The retina undergoes progressive degeneration with the ventral retina more severely affected than the dorsal retina. Cygb expression is in neurons of the retinal ganglion cell layer and inner nuclear layer. Immunohistochemical studies suggest that cell death predominates in the photoreceptors. Electroretinography amplitudes show reduced a- and b-waves, consistent with photoreceptor disease. Cygb deficient retinas had only modest transcriptional perturbations of Crb1-related cell polarity genes. Cygb$^{-/-}$mice without the *rd8* mutation did not exhibit obvious retinal abnormalities. Conclusions: Cygb is necessary for retinal lamination, maintenance of cell polarity, and photoreceptor survival in *rd8* mice. These results are consistent with Cygb as a disease modifying gene in Crb1-related retinopathy. Further studies are necessary to investigate the role of Cygb in the human retina.

Introduction

Maintenance of cell polarity is a critical function in all polarized cells. In the mammalian retina, photoreceptors and the retinal pigment epithelium (RPE) both require appropriate cell polarity in order to keep their intercellular connections and directional transport of cellular materials.[1] Proteins in the Crumbs (Crb) family are present and conserved between many species including humans, rodents, fish, and fruit flies.[2] The drosophila *Crumbs* mutant results in loss of the cuticle in the embryo, with preservation of a few residual grains resembling crumbs.[3] Humans and rodents have *Crumbs* homologues in the form of Crb1, Crb2, and Crb3. The expression of Crb1 is restricted to the central nervous system,[4] while Crb2 and Crb3 are expressed in the retina, heart, lung, kidneys, and other tissues.[5,6] Crb1 is expressed in the subapical region (SAR) of Muller glia and photoreceptors and is critical for the maintenance and integrity of the outer limiting membrane (OLM). The OLM is formed by Muller glial apical villi which form adherens junctions with photoreceptors through a group of adapter proteins, which include Crb1 and Crb2. Two protein complexes regulating cell polarity reside on the apical side of the adherens junctions in both Muller glia and photoreceptors: the Crumbs-homologue (CRB) complex and the partitioning defective (PAR) complex.

Mutations in the Crumbs homolog 1 (*CRB1*) gene cause Leber's congenital amaurosis and retinitis pigmentosa in humans.[7] It has also been implicated in Coat's disease,[8] pigmented paravenous chorioretinopathy,[9] and nanopthalmos and optic nerve drusen.[10] However, the relatively broad range in phenotypes has not been explained by differences in the location or nature of mutations within *CRB1*. This suggests that modifying genes (and/or environmental effects) may play significant roles in determining the disease phenotype in various individual patients.[11,12,13] Therefore, elucidation of the molecular underpinnings surrounding these phenotypic variabilities is important both for understanding retinal biology and for developing patient treatment strategies.

Several mouse models exist for studying *CRB1*-related eye diseases, including Crb1$^{-/-}$ mice,[14] CrbC^{294W} (knock-in) mice,[15] and the spontaneously occurring retinal degeneration 8 (*rd8*) mouse.[16] The *rd8* mouse contains a single nucleotide deletion in *Crb1* causing a frameshift mutation and early termination. The consequences of this mutation have been extensively characterized. Its retina has focal yellow spots that tend to occur inferiorly and

correspond to dysplastic retinal folds and pseudorosettes.[17] These lamination defects likely represent aberrant cell polarity between progenitor cells, Muller glia, and newborn photoreceptors during retinal development. These mice subsequently undergo a slow and progressive photoreceptor degeneration. Despite the cell polarity abnormalities described, the photoreceptors are functional, as is evidenced by the preserved electroretinogram (ERG) through postnatal month 18, though b-wave amplitudes decline thereafter.[18]

In order to identify modifying genes which may regulate Crb1-associated retinopathies we can study mice with targeted genetic deletions on the *rd8* background. The International Mouse Phenotyping Consortium (IMPC) uses C57BL/6N mice homozygous for the *rd8* mutation to produce single gene knockouts.[19] As part of our efforts to screen knockout mice created for the IMPC at the UC Davis Mouse Biology Program, we discovered that the fundus in mice deficient in Cytoglobin ($Cygb^{-/-rd8/rd8}$) had more severe abnormalities than the fundus in C57BL/6N *rd8* ($Cygb^{+/+rd8/rd8}$) control mice.[20] Cytoglobin, discovered in 2001,[21] is a heme-containing protein that is a member of the globin family and is thought to protect against hypoxia by acting as a local oxygen (O_2) reservoir, to reduce oxidative stress by scavenging reactive oxygen species (ROS), and also to regulate nitric oxide (NO) levels through dioxygenase activity.[22,23] Cygb binds iron in a hexacoordinate fashion involving the imidazole groups of histidine residues.[24] $Cygb^{-/-}$ mice are prone to developing liver cancer when exposed to carcinogens[25] or in a model of steatohepatitis.[26] Aged $Cygb^{-/-}$ mice develop various forms of tumors and other solid organ abnormalities as they age, as well as increased NO metabolites in their urine.[27] Cytoglobin is expressed in the central nervous system and retina,[28,29] and co-localizes with neurons expressing neuronal nitric oxide synthase (nNos).[30] The role of Cygb in controlling the severity of Crb1-related retinal degeneration, therefore, may shed light on genetic pathways relevant in Crb1-related retinal diseases and explain, in part, the diversity of phenotypes seen in affected patients.

Results

Deletion of Cygb on the C57BL/6N background worsens the photoreceptor lamination defects seen in *rd8* mice

Cytoglobin knockout mice were generated on the C57BL/6N strain, homozygous for the *rd8* mutation, at the UC Davis Mouse Biology Program as part of the Knockout Mouse Phenotyping (KOMP) project. $Cygb^{-/-\ rd8/rd8}$ mice were initially phenotyped at 15–16 weeks postnatal age by a trained veterinary ophthalmologist (SE) and determined to have retinal fundus hyperpigmentation (Figure 1 C). $Cygb^{-/-\ rd8/rd8}$ mice were found to have numerous white spots in the inferior retina even at 1-month postnatal age (Figure 1 A) which become nearly confluent by 2 months (Figure 1 B). At four months of age, the inferior retina appears hyperpigmented and atrophic (Figure 1 C), and spots developed in the superior retina (Figure 1 C, arrowheads). Cygb heterozygosity in the context of homozygous *rd8* mutation (Figure 1 D, E, F) did not result in significantly more numerous spots or a progressively degenerate retinal fundus phenotype when compared to C57BL/6N mice with the *rd8* mutation alone (Figure (G, H, I) at the ages examined. Quantification of the ventral retinal changes seen in $Cygb^{-/-\ rd8/rd8}$ mice are shown in Supplemental Figure 1.

In order to non-invasively interrogate the retinal architecture of $Cygb^{-/-\ rd8/rd8}$ mice, we used optical coherence tomography (OCT) of mice at various ages. We specifically targeted the area of the white spots in the inferior retina. The green line in Figure 2 A' corresponds to the cross-sectional image in panel 2 A. The retina of $Cygb^{-/-rd8/rd8}$ mice shows outer retinal hyperreflective lesions and loss of outer retinal bands. Areas of hyperreflectivity are seen as early as postnatal month 1 (Figure 2 A, arrows), and persist at postnatal month 2 (Figure 2 B, arrows) and 4 (Figure 2 C, arrows). Similar lesions are occasionally seen in $Cygb^{+/+rd8/rd8}$ animals (Figure 2 D, E, F) at these ages (arrow in E), but to a lesser degree. The outer retinal bands (Figure 2 D, E, F, arrowheads) representing the external limiting membrane, the inner segment/outer segment junction (aka ellipsoid zone), and the retinal pigmented epithelium are not discernible in $Cygb^{-/-rd8/rd8}$ mice (Figure 2 A, B, C arrowheads). In addition, the total thickness decreases with age in $Cygb^{-/-rd8/rd8}$ mice (Figure 2 A, B, C), suggesting the presence of an active degenerative process.

In order to investigate the cellular abnormalities due to Cygb deficiency at the cellular level, we performed retinal histology at various stages. We found that $Cygb^{-/-rd8/rd8}$ mice have an increase in the severity of photoreceptor lamination defects when compared to *rd8* control mice. At several postnatal ages, and as early as postnatal day 14, hematoxylin and eosin histological analysis of the outer nuclear layer in $Cygb^{-/-rd8/rd8}$ retina (Figure 3 A–C) reveals profound outer retinal lamination defects. We observed photoreceptor rosettes that were larger and more numerous than those seen in $Cygb^{+/+rd8/rd8}$ mice (Figure 3 bar graph). The outer nuclear layer eventually had areas of photoreceptor loss (Figure 3 D). By contrast, $Cygb^{+/+rd8/rd8}$ mice (Figure 3 E–H) have smaller and less numerous lamination defects without obvious cell loss at these time points.

Deletion of Cygb on the C57BL/6N background accelerates the retinal degeneration seen in *rd8* mice

The mutation in Crb1 leads to slowly progressive photoreceptor loss and thinning of the outer nuclear layer in aged *rd8* mice. Deficiency of Cygb accelerates the photoreceptor loss. At 24 months postnatal age, $Cygb^{-/-rd8/rd8}$ moderate (Figure 4 B), and mild (Figure 4 C) mice have areas of severe (Figure 4 A), retinal degeneration within the same eye. The variability observed within each retina of these mice are attributed to the inferior to superior pattern of severity seen on fundus examination. The $Cygb^{+/+rd8/rd8}$ littermates (Figure 4 D–F) have areas of normal to mild retinal degeneration in this aged cohort. The dorsal and ventral extent of outer retinal lamination defects is quantified in Supplemental Figure 1.

In order to determine the degree of retinal function preserved in $Cygb^{-/-rd8/rd8}$ mice, we performed electroretinography at various ages. We found that rod retinal function declines with age in $Cygb^{-/-rd8/rd8}$ mice. Scotopic (dark-adapted) and photopic (light-adapted) electroretinography was performed in $Cygb^{-/-rd8/rd8}$ mice and $Cygb^{+/+rd8/rd8}$ controls at one (Figure 5 A), 2 (Figure 5 B), 4 (Figure 5 C), and 24 (Figure 5 D) months postnatal age. Representative wave forms are shown (Supplemental Figure 2). We plotted stimulus-response curves demonstrating the absolute values of the a- and b-waves for $Cygb^{-/-rd8/rd8}$ (solid line) and $Cygb^{+/+rd8/rd8}$ (dashed line) mice on the same graphs. At 1- and 2-months postnatal age (Figure 5 A, B), rod and cone mediated retinal pathways appear similar in both

groups. However, by 4 months of age (Figure 5 C) the scotopic b-wave begins to decline in Cygb$^{-/-rd8/rd8}$ mice when compared to Cygb$^{+/+rd8/rd8}$ controls. The reduced retinal function at 4 months corresponds to the time of substantial retinal degeneration seen on fundus photos, OCT, and histology. By 24 months postnatal age, the scotopic b-wave is markedly reduced in Cygb$^{-/-rd8/rd8}$ mice in comparison to *rd8* littermates. Interestingly, photopic responses appear similar at all stages in both groups, suggesting less involvement of the cone-mediated responses.

Cygb is required for maintenance of photoreceptor lamination and survival

By taking advantage of several methods we found that Cygb is not expressed in photoreceptors, but rather in the inner retina. Immunohistochemistry at postnatal age 1 month using anti-ß-galactosidase antibodies as a surrogate for Cygb expression (Figure 6 A) shows protein expression in the retinal ganglion cell layer and the inner aspect of the inner nuclear layer. Antibodies against Cygb (Figure 6 B) showed a pattern consistent with the expression of ß-galactosidase at the same age. We also used LacZ histochemistry, which corroborates this inner retinal expression pattern in postnatal day 14 Cygb heterozygous mice (Figure 6 C, left panel), and in neonatal heterozygous mice at postnatal day 3 (Figure 6 C, right panel). We found a similar pattern of Cygb expression by immunohistochemistry at P0, P10, and 1 month postnatal in wild type mice without the rd8 mutation (Supplemental Figure 3). To determine the role of Cygb in retinal development, we checked for Cygb expression in retinal progenitor cells (Supplemental Figure 4). We found Cygb expressed in post-mitotic neurons of the inner retina, but not in retinal progenitors. In an effort to identify the cells expressing cytoglobin, we performed co-labeling experiments with Cygb and retinal cell-type specific markers. We found that Cygb is expressed in retinal ganglion cells and amacrine cells. Double-labeling at postnatal age 1-month using (Figure 7 A–D) anti-Cygb and anti-Brn3, a nuclear marker restricted to retinal ganglion cells, showed co-labeling in cells of the retinal ganglion cell layer. Similarly, anti-Cygb and anti-AP2, a nuclear amacrine cell marker (Figure 7 E–H), were found to coincide in the inner nuclear layer. We found that Cygb is localized both to the cytoplasmic and nuclear compartments in these neurons. To test the possibility that Cygb could be expressed in Muller glia, we performed co-labeling experiments with anti-Vimentin and anti-Cygb antibodies in WT mice, and also co-labeling experiments with anti-ßgal and anti-Sox9 antibodies in Cygb $^{+/-}$ mice (Supplemental Figure 5). We did not see expression of Cygb in Muller glia.

GFAP immunoreactivity indicating areas of reactive Muller glia is shown in (Figure 8 A) Cygb$^{+/+rd8/rd8}$ mice and (Figure 8 B) Cygb$^{-/-rd8/rd8}$ mice at postnatal age 2 months. Cygb $^{-/-rd8/rd8}$ demonstrate more GFAP immunoreactivity than Cygb$^{+/+rd8/rd8}$ controls, and the areas of reactive Muller glia correspond to the loci of outer nuclear layer lamination defects. Since *rd8* mice are known to have (OLM) abnormalities, we sought to determine the degree to which Cygb deficiency results in disruption of this outer retinal structure. We used anti-ZO1 to evaluate the integrity of the OLM. The OLM as stained by anti-ZO1 immunohistochemistry shows relative preservation of this structure in (Figure 8 C) Cygb $^{+/+rd8/rd8}$ mice, but with frequent areas of discontinuity seen in (Figure 8 D) Cygb$^{-/-rd8/rd8}$ mice at postnatal age 3 weeks. Virtually no anti-activated Caspase 3 staining is seen at postnatal age 4 months in (Figure 8 E) the Cygb$^{+/+rd8/rd8}$ retina, while robust staining of this

apoptotic marker is seen in the outer nuclear layer at this age in (Figure 8 F) Cygb$^{-/-rd8/rd8}$ mice.

Cygb is not required for appropriate transcriptional regulation of cell polarity genes

To test the hypothesis that Cygb is required for transcriptional regulation of cell polarity genes, we used quantitative PCR to compare the relative levels of mRNA from 17 cell polarity genes (Table 1) associated with the Crb cell polarity complex. Quantitative PCR from cDNAs derived from Cygb$^{-/-}$ and wild type retinas at age 1 month were used (primers shown in Table 2). In order to test the direct effect of Cygb deficiency in the context of a healthy retina, we used mice free from the *rd8* mutation (Cygb$^{-/-}$ compared to WT littermate controls). To understand the effect of Cygb deficiency on gene expression in the context of *rd8*, we also compared cDNAs derived from Cygb$^{-/-rd8/rd8}$ mice and compared them to Cygb$^{+/+rd8/rd8}$ littermate mice. We found that expression of 12 Crb-related genes was modestly reduced at the transcriptional level in retinas from Cygb$^{-/-}$ mice compared to WT controls (Table 1). However, no transcriptional alterations were found in Cygb$^{-/-rd8/rd8}$ mice when compared to Cygb$^{+/+rd8/rd8}$ controls (Table 1). To test the potential role of Nitric Oxide signaling in the Cygb$^{-/-}$ retina, we performed qPCR on three genes downstream of NO signaling (Hpn, Pea15a, Rprm). Rprm transcription is induced in response to NO pathway activation, while Hpn and Pea15a are repressed. No significant differences were detected in the transcription of Rprm in any genotype. Consistent with Cygb inhibiting NO signaling through NO metabolism, we found that Hpn and Pea15a were repressed in Cygb$^{-/-}$ mice. However, no differences were detected in Cygb$^{-/-rd8/rd8}$ mice. We then tested two oxidative stress genes, Aass and Gpx1, whose transcription was repressed in Cygb$^{-/-}$ liver.[26] We found that Aass and Gpx1 transcription was reduced in Cygb$^{-/-}$ retinas, though only significantly for Gpx1, while Aass approached statistical significance (P=0.068). When we tested the same two oxidative stress genes in Cygb$^{-/-rd8/rd8}$ mice, we found reduced transcription in Aass.

Cygb$^{-/-}$ mice without the *rd8* mutation have no obvious retinal abnormalities

In spite of modestly altered transcription of Crb-associated cell polarity genes, Cygb knockout mice free from the *rd8* mutation had no obvious retinal abnormalities at postnatal age 4 months. Color fundus photos of wild type and Cygb$^{-/-}$ mice on the C57BL/6J background confirmed to be free of the *rd8* mutation were indistinguishable at 4 months postnatal age (Figure 9 A and B). Spectral domain optical coherence tomography (SD-OCT) of wild type and Cygb$^{-/-}$ mice showed similar retinal lamination (Figure 9 C and D), which is consistent with the hematoxylin and eosin histological analysis at 4 months postnatal (Figure 9 E and F).

Discussion

Cygb deficiency worsens the Crb1 retinal phenotype

The data presented in this report demonstrate that Cygb is linked, directly or indirectly, with Crb1-mediated cell polarity in the retina. In the absence of cytoglobin, the cell polarity defects in *rd8* mice are more severe. Rosette formation in the outer nuclear layer is increased by nearly ten-fold soon after retinal histogenesis, likely representing a profound

developmental defect in cell polarity of photoreceptors. It is known that mice with Crb1 deficiency have a relatively modest retinal degeneration compared to human counterparts. Hypotheses to explain this disparity include possible differences in the cellular expression of Crb1 in mouse and human retina, and the possibility of genetic modifiers contributing to Crb1-associated retinopathies in humans. Crb2 is thought to compensate for the loss of Crb1 in mice. Consistent with this concept is the more severe retinal degeneration phenotype in mouse retinas lacking Crb2, mimicking Crb1-associated retinitis pigmentosa in people.[31] $Crb1^{-/-}$:$Crb2^{-/-}$ double knockout mice exhibit a more severe retinal degeneration phenotype than that from loss of Crb2 alone and is analogous to LCA in humans.[32] Crb1 and Crb2 are transmembrane proteins expressed on the apical side of polarized cells in the retina. The adherens junctions forming the OLM are comprised of Crb2 expressed in Muller glia and photoreceptors, and Crb1 expressed in Muller glia alone.[33] The cytosolic side of these proteins interacts with a series of proteins that comprise the Crb1 cell-polarity complex. Genetic models of several of these cell-polarity complex factors result in retinal dysplasia and/or degeneration. These animal models of retinal disease include mutations in Mpp3[34,35], Mpp5 (aka Pals1)[36,37,38], aPKC[39], Cdc42[40], Aspp2[41], and Mpdz[42,43]. With the exception of Crb1 and Crb2, compound knockouts of these genes have not been published, and it is plausible that this would increase the severity of the Crb1 phenotype. A patient with CRB1-associated LCA was identified with a mutation in one copy of AIPL1.[44] Similarly, a CRB1 mutation in one allele has been identified in an LCA patient attributed to biallelic AIPL1 mutations.[45] CRB2 monoallelic variants have been identified in patients with presumed inherited retinal disease.[46] Crb2 germline knockout mice are lethal,[47] and the same may be true of humans, suggesting heterozygous alterations in CRB2 may be relevant to the presence and/or severity of inherited retinal disease. Genetic analysis of patients with two mutations in the CRB1 gene are necessary to identify modifying genes.

Cygb does not strongly regulate transcription of Crb-related cell polarity genes

The mechanism by which Cygb worsens the *rd8* retinal phenotype is unclear, since Cygb is neither expressed in Muller glia nor photoreceptors. The anatomical discordance between Cygb and Crb1 expression implies a cell non-autonomous mechanism of action between cells expressing these genes. Cygb protein is known to localize to not only the cytosol, but in some contexts also in the nucleus.[48,49] Therefore, we tested whether or not transcriptional regulation of genes in the Crb1-related cell polarity complex were altered in the absence of Cygb. We found that 12 genes (Crb2, Cdc42, Prkci, Prkcz, Pard6a, Pard6b, Pard6g, Pard3, RacGap1, Mpp5, Lin7a, Mpdz) were downregulated in the absence of Cygb. It is feasible that alterations in these transcripts are sufficient to worsen the retinal dysplasia phenotype in *rd8* mice. However, no alterations in transcriptional levels of any cell polarity genes were detected in the context of *rd8* mutation ($Cygb^{-/-rd8/rd8}$ vs $Cygb^{+/+rd8/rd8}$ controls). Mpdz knockout mice undergo severe retinal degeneration.[50] Crb2 is implicated in retinal disease (Alves 2013).[31] In the mouse retina Crb1 is expressed in Muller glia, while Crb2 is expressed in Muller glia and photoreceptors. Crb1 deficiency causes retinal dysplasia secondary to developmental cell polarity defects, followed by a slow retinal degeneration in mice. Crb2 deficiency in the mouse retina causes more severe developmental defects including major abnormalities in lamination, cell fate specification, and cell survival. $Crb1^{-/-}$;$Crb2^{-/-}$ mice have a more severe retinal phenotype than Crb1 deficient mice.

Therefore, it is likely that Crb2 expression partially compensates for the absence of Crb1 in the retina. Misregulation of Crb2 in the $Cygb^{-/-}$ retina may explain the more severe phenotype in *rd8* mice, implying an indirect Cygb-dependent transcriptional mechanism for Crb2 compensation of Crb1 deficiency. However, the fact that no transcriptional differences in cell polarity genes were evident in the context of *rd8* deficiency ($Cygb^{-/-rd8/rd8}$ vs $Cygb^{+/+rd8/rd8}$ controls) calls into question the degree to which altered regulation of cell polarity genes in compound mutants is responsible for the more severe phenotype. Cygb is not known to be a transcription factor, and any alterations in the transcription of cell polarity genes are likely indirect effects of Cygb deficiency.

Putative functions of Cygb in the retina

How does Cygb control transcription of cell polarity genes in adjacent cells? The cell non-autonomous mechanism by which Cygb affects transcription of these genes is presumably through intercellular signaling. Cygb is not known to be required for or tightly linked to any cellular growth factors or peptide signaling molecules. In the central nervous system, Cygb expression is known to correlate strongly with cells expressing neuronal nitric oxide synthase.[51] The strength of this correlation throughout many parts of the brain strongly implies a mechanistic relationship. Cygb, like other globins, is known to bind O2 and other diatomic gases such as NO and carbon monoxide (CO).[52,53,54] Consistent with the idea that Cygb is involved in NO metabolism, it has been reported that Cygb reduces local NO concentrations through dioxygenase activity.[55,56,57] Furthermore, Cygb deficient animals have systemic hypotension and vasodilatation secondary to decreased circulation NO (Liu et al).[23] Consistent with the concept that the $Cygb^{-/-}$ retina may have increased NO levels, we measured reductions in Hpn and Pea15a transcripts, genes repressed by NO signaling. However, we did not make similar observations in the $Cygb^{-/-rd8/rd8}$ retina. We cannot definitively conclude that loss of retinal Cygb by itself potentiates the phenotype of rd8 mice. Physiologic changes owing to systemic loss of Cygb in this germline mutant model may be responsible for our observations. Since Cygb is known to bind oxygen like other globins, we cannot exclude the hypothesis that Cygb may serve as an O_2 reservoir in the retina and may be critical to mitochondrial function in this highly metabolic tissue.[58,59] Similarly, Cygb binds reactive oxygen species to scavenge free radicals and protects against oxidative stress.[60,61] Consistent with this hypothesis, we found alterations in the oxidative stress genes Aass and Gpx1. The function of Cygb in retinal cells may indeed involve ROS scavenging, and may potentiate retinal degenerations in a non-specific manner. None of these functions are mutually exclusive, and further studies are needed to determine the degree to which Cygb participates in each of these functions in the retina.

While over 150 different mutations in the Cygb gene have been detected in patients with inherited retinal disease, there is no clear genotype-phenotype correlation.[62] Cytoglobin, while it does not localize to the OLM and does not participate directly in the formation of cell polarity complexes in the outer retina, may represent a disease modifying locus by indirect transcriptional regulation of cell polarity complex genes. Further studies will determine the relative clinical importance of Cytoglobin in Crb1-associated retinopathies.

Materials and Methods

This study was conducted according to a protocol (#19494) that was approved by the Institutional Animal Care and Use Committee at the University of California Davis and was compliant with the ARVO Statement for the Use of Animals in Ophthalmic and Vision Research.

Animals

Mice were engineered and a breeding colony established at the U.C. Davis Mouse Biology Program as part of the KOMP/IMPC project and were transferred to and maintained at the Animal Facility at the University of California Davis where a breeding colony was established. A targeting cassette with a *LacZ* insert was used to knock out exon 2 of the Cygb gene. Homozygous male and female cohorts of adult Cygb1$^{-/-}$ mice were generated on a C57BL/6N background, which commonly carries homozygous mutations at the rd8 locus in the Crb1 gene, confirmed by genotyping as previously described (Mattapallil et al 2012). At the outset of this study Cygb$^{-/-\ rd8/rd8}$ founders were crossed to C57BL/6J mice confirmed to be free of the rd8 mutation for several generations. Cygb$^{-/-}$ mice on the C57BL/6J background were then crossed back onto the C57BL/6N background for several generations in order to minimize the possibility of genetic confounders producing the phenotypic observations. All animals used in this study are the product of this outcrossing process. Primers flanking the engineered deletion in the Cygb gene were used for genotyping mutant alleles, and primers within the deletion were used to amplify wild type alleles.

Electroretinography

ERG was performed on one eye of some animals just before euthanasia. Mice were dark adapted overnight just before ERG testing (UTAS–EPIC XL; LKC Technologies, Gaithersburg, MD). Mice were then anesthetized intraperitoneally with a 0.1 mL/10 g dose of a ketamine (100 mg/mL to 1 mL) and xylazine (100 mg/mL to 0.1 mL) cocktail diluted 1:10 in sterile saline. After administration of anesthesia, mice were placed on a heating pad set at 38°C and one eye dilated with 1% tropicamide and 2.5% phenylephrine. Proparacaine eye drops were applied for topical anesthesia. The eyes were lubricated with 1% methylcellulose. Mouse contact lens electrodes (LKC Technologies) were then placed on each eye, needle reference electrodes were placed in each cheek, respectively, and finally a ground needle electrode was placed at the base of the tail. ERGs were generated with the following program: scotopic blue filter (0 dB) at 20 μV/div single flash; scotopic white (0 dB) at 50 μV/div single flash; photopic white (0 dB) 10 μV/div single flash; and photopic white (0 dB) 20 μV/div flicker, average of 10.

Immunohistochemistry

All eyes for immunohistochemical analysis were perforated with a 30-gauge needle and immersion fixed in 4% (w/v) buffered paraformaldehyde (PFA) for 30 minutes, then washed in three changes of PBS. The procedure for immunohistochemical analysis was similar to a method previously described.[63] The eyes were dehydrated in a 10–20-30% sucrose gradient and then embedded in OCT medium for cryosectioning. Sections (10 μm thickness) were

collected, and attention was paid to use retinal sections at or near the level of the optic nerve. The sections were then immersed in blocking solution, PBS containing 1% (w/v) bovine serum albumin (BSA) with 0.3% Triton X-100. The sections were then reacted (with appropriate washes between incubations) with primary antibodies at 4 degrees overnight. The next day, slides were washed, and species-specific fluorescent tagged secondary antibodies were applied for 30 minutes at room temperature. Sections incubated without primary antibody, but with secondary antibody, were used as controls. The slides were then washed and mounted with commercial antifade medium (Vectashield; Vector Laboratories, Burlingame, CA) and digital image captures were made with an epifluorescence microscope (Zeiss Axioplan 2; Carl Zeiss, Inc., Thornwood, NY) coupled to a charge-coupled device camera (SPOT Imaging Solutions, Division of Diagnostic Instruments, Inc., Sterling Heights, MI). Primary antibodies used in this study include rabbit anti-activated Caspase 3 (BD Biosciences), rabbit anti-Cygb (Santa Cruz), mouse anti- ß gal (Developmental Studies Hybridoma Bank, Iowa), goat anti-Brn3 (Santa Cruz), mouse anti-AP2 (DSHB), rabbit anti-ZO1 (Invitrogen), rabbit anti-GFAP (DakoCytomation), rabbit anti-Sox9 (Millipore), chicken anti-Vimentin (generous gift from Paul Fitzgerald), mouse anti-PCNA (ThermoFisher), and rabbit anti-Ki67 (ThermoFisher). Species-specific secondary antibodies conjugated to Alexa-Fluor 488 or −594 (Invitrogen) were used.

Quantitative Polymerase Chain Reaction (qPCR)

Eyes were enucleated and then the retina was dissected and immediately placed in RNAlater Stabilization Solution (Ambion). Retinas were then stored in at 4°C overnight before moving into a −20°C freezer to be stored until RNA was extracted. RNA extraction was done using a Zymo Quick-RNA Mini Prep Kit (Zymo Research). RNA concentrations were measured using a Qubit 4 Fluorometer (Qubit Q33226). RNA was then transcribed to cDNA using an iScript cDNA Synthesis Kit (Bio-Rad). After synthesis, cDNA was diluted 1:25 using milli-q water and stored at −20°C. qPCR was performed on a StepOnePlus Real-Time PCR System (Applied Biosystems) using Fast SYBR Green Master Mix (Applied Biosystems). 96-well plates containing gene-specific primers (Table 1) were tested on three biological replicates of cDNA derived from wild-type and Cygb knockout retinas. Each primer was tested at least three times (technical replicates) for each sample. Results were analyzed using the ΔΔCt method to determine the fold-change. Two-tailed students *t*-test was used to compare each gene between the two groups. *P*-values < 0.05 were considered statistically significant.

Histology

Mice were euthanized by isoflurane inhalation followed by cervical dislocation. Eyes were enucleated and then immediately fixed using freeze substitution and embedded in paraffin as previously described.[64] Eyes were sectioned at 5 μm on a microtome and sections collected on slides and dried. Using standard protocols, sections were treated with cold acetone, hematoxylin, 0.5% HCl in 70% ethanol, eosin, 95% and 100% ethanol and Histo-Clear for light microscopic examination.

LacZ histochemistry

Retinal sections which had been previously fixed for 30 minutes in PFA 4% and sectioned at 10 μm thickness were defrosted, rinsed in PBS twice, and sections circled with a grease pen. Sections were covered in X-gal stain[65] and incubated in dark at 37°C up to 8 hours if necessary until blue pigment was detected in LacZ expressing tissue slides, but not in control slides. Slides were washed again in PBS twice, and coverslipped.

Statisitics and Quantification

Quantification of lamination defects were performed on H&E sections of retina at the level of the optic nerve. We counted and averaged all lamination defects from 3 retinal sections from each of 3 biological replicates from each genotype. A similar strategy was performed when counting GFAP-positive complexes of activated Muller glia, outer nuclear layer thickness, and linear percentage of retina with lamination defects in the dorsal versus ventral retina. White spots were counted from one fundus photo taken from one eye of each animal, based on image quality, and averaged between genotypes.

Quantitative comparisons between two genotypes, $Cygb^{-/-\ rd8/rd8}$ and $Cygb^{+/+\ rd8/rd8}$ were assessed for statistical significance using a two-tailed student's *t*-test in all instances. For quantitative PCR comparisons, the results were analyzed using the ΔΔCt method to determine the fold-change. The two-tailed students *t*-test was used to compare each gene between the two groups. For qPCR, $Cygb^{-/-\ rd8/rd8}$ was compared with $Cygb^{+/+\ rd8/rd8}$ controls. $Cygb^{-/-}$ mice were compared with WT controls. In all experimental quantifications reported in this study *P*-values < 0.05 were considered statistically significant, and all error bars shown represent standard error of the mean.

Supplementary Material

Refer to Web version on PubMed Central for supplementary material.

References

1. Gosens I, den Hollander AI, Cremers FP, Roepman R. Composition and function of the Crumbs protein complex in the mammalian retina. Exp Eye Res 2008 5; 86(5):713–26. [PubMed: 18407265]
2. Tepass U, Theres C, Knust E. crumbs encodes an EGF-like protein expressed on apical membranes of Drosophila epithelial cells and required for organization of epithelia. Cell 1990 6 1; 61(5):787–99. [PubMed: 2344615]
3. Grawe F, Wodarz A, Lee B, Knust E, Skaer H. The Drosophila genes crumbs and stardust are involved in the biogenesis of adherens junctions.Development 1996 3; 122(3):951–9. [PubMed: 8631272]
4. den Hollander AI, Heckenlively JR, van den Born LI, de Kok YJ, van der Velde-Visser SD, Kellner U, Jurklies B, van Schooneveld MJ, Blankenagel A, Rohrschneider K, Wissinger B, Cruysberg JR, Deutman AF, Brunner HG, Apfelstedt-Sylla E, Hoyng CB, Cremers FP. Leber congenital amaurosis and retinitis pigmentosa with Coats-like exudative vasculopathy are associated with mutations in the crumbs homologue 1 (CRB1) gene. Am J Hum Genet 2001 7; 69(1):198–203. [PubMed: 11389483]
5. van den Hurk JA, Rashbass P, Roepman R, Davis J, Voesenek KE, Arends ML, Zonneveld MN, van Roekel MH, Cameron K, Rohrschneider K, Heckenlively JR, Koenekoop RK, Hoyng CB, Cremers FP, den Hollander AI. Characterization of the Crumbs homolog 2 (CRB2) gene and analysis of its

role in retinitis pigmentosa and Leber congenital amaurosis. Mol Vis 2005 4 15; 11():263–73. [PubMed: 15851977]

6. Makarova O, Roh MH, Liu CJ, Laurinec S, Margolis B. Mammalian Crumbs3 is a small transmembrane protein linked to protein associated with Lin-7 (Pals1). Gene 2003 1 2; 302(1–2): 21–9. [PubMed: 12527193]
7. den Hollander AI, Davis J, van der Velde-Visser SD, Zonneveld MN, Pierrottet CO, Koenekoop RK, Kellner U, van den Born LI, Heckenlively JR, Hoyng CB, Handford PA, Roepman R, Cremers FP. CRB1 mutation spectrum in inherited retinal dystrophies. Hum Mutat 2004 11; 24(5):355–69. [PubMed: 15459956]
8. Richard M, Roepman R, Aartsen WM, van Rossum AG, den Hollander AI, Knust E, Wijnholds J, Cremers FP. Towards understanding CRUMBS function in retinal dystrophies. Hum Mol Genet 2006 10 15; 15 Spec No 2():R235–43. [PubMed: 16987889]
9. McKay GJ, Clarke S, Davis JA, Simpson DA, Silvestri G. Pigmented paravenous chorioretinal atrophy is associated with a mutation within the crumbs homolog 1 (CRB1) gene. Invest Ophthalmol Vis Sci 2005 1; 46(1):322–8. [PubMed: 15623792]
10. Paun CC, Pijl BJ, Siemiatkowska AM, Collin RW, Cremers FP, Hoyng CB, den Hollander AI. A novel crumbs homolog 1 mutation in a family with retinitis pigmentosa, nanophthalmos, and optic disc drusen. Mol Vis 2012;18:2447–53. [PubMed: 23077403]
11. Bujakowska K, Audo I, Mohand-Saïd S, Lancelot ME, Antonio A, Germain A, Léveillard T, Letexier M, Saraiva JP, Lonjou C, Carpentier W, Sahel JA, Bhattacharya SS, Zeitz C. CRB1 mutations in inherited retinal dystrophies. Hum Mutat 2012 2; 33(2):306–15. [PubMed: 22065545]
12. Henderson RH, Mackay DS, Li Z, Moradi P, Sergouniotis P, Russell-Eggitt I, Thompson DA, Robson AG, Holder GE, Webster AR, Moore AT. Phenotypic variability in patients with retinal dystrophies due to mutations in CRB1. Br J Ophthalmol 2011 6; 95(6):811–7. [PubMed: 20956273]
13. Luhmann UF, Carvalho LS, Holthaus SM, Cowing JA, Greenaway S, Chu CJ, Herrmann P, Smith AJ, Munro PM, Potter P, Bainbridge JW, Ali RR. The severity of retinal pathology in homozygous Crb1rd8/rd8 mice is dependent on additional genetic factors. Hum Mol Genet 2015 1 1; 24(1): 128–41. [PubMed: 25147295]
14. van de Pavert SA, Kantardzhieva A, Malysheva A, Meuleman J, Versteeg I, Levelt C, Klooster J, Geiger S, Seeliger MW, Rashbass P, Le Bivic A, Wijnholds J. Crumbs homologue 1 is required for maintenance of photoreceptor cell polarization and adhesion during light exposure. J Cell Sci 2004 8 15; 117(Pt 18):4169–77. [PubMed: 15316081]
15. van de Pavert SA, Meuleman J, Malysheva A, Aartsen WM, Versteeg I, Tonagel F, Kamphuis W, McCabe CJ, Seeliger MW, Wijnholds J. A single amino acid substitution (Cys249Trp) in Crb1 causes retinal degeneration and deregulates expression of pituitary tumor transforming gene Pttg1. J Neurosci 2007 1 17; 27(3):564–73. [PubMed: 17234588]
16. Chang B, Hawes NL, Hurd RE, Davisson MT, Nusinowitz S, Heckenlively JR. Retinal degeneration mutants in the mouse. Vision Res 2002 2; 42(4):517–25. [PubMed: 11853768]
17. Mehalow AK, Kameya S, Smith RS, Hawes NL, Denegre JM, Young JA, Bechtold L, Haider NB, Tepass U, Heckenlively JR, Chang B, Naggert JK, Nishina PM. CRB1 is essential for external limiting membrane integrity and photoreceptor morphogenesis in the mammalian retina. Hum Mol Genet 2003 9 1; 12(17):2179–89. [PubMed: 12915475]
18. Aleman TS, Cideciyan AV, Aguirre GK, Huang WC, Mullins CL, Roman AJ, Sumaroka A, Olivares MB, Tsai FF, Schwartz SB, Vandenberghe LH, Limberis MP, Stone EM, Bell P, Wilson JM, Jacobson SG. Human CRB1-associated retinal degeneration: comparison with the rd8 Crb1-mutant mouse model. Invest Ophthalmol Vis Sci 2011 8 29; 52(9):6898–910. [PubMed: 21757580]
19. Mattapallil MJ, Wawrousek EF, Chan CC, Zhao H, Roychoudhury J, Ferguson TA, Caspi RR. The Rd8 mutation of the Crb1 gene is present in vendor lines of C57BL/6N mice and embryonic stem cells and confounds ocular induced mutant phenotypes. Invest Ophthalmol Vis Sci 2012; 53(6): 2921–7. [PubMed: 22447858]
20. Moore BA, Roux MJ, Sebbag L, Cooper A, Edwards SG, Leonard BC, Imai DM, Griffey S, Bower L, Clary D, Lloyd KCK, Hérault Y, Thomasy SM, Murphy CJ, Moshiri A. A Population Study of

Common Ocular Abnormalities in C57BL/6N rd8 Mice. Invest Ophthalmol Vis Sci 2018 5 1;59(6):2252–2261. [PubMed: 29847629]

21. Kawada N, Kristensen DB, Asahina K, Nakatani K, Minamiyama Y, Seki S, Yoshizato K. Characterization of a stellate cell activation-associated protein (STAP) with peroxidase activity found in rat hepatic stellate cells. J Biol Chem 2001 7 6;276(27):25318–23. [PubMed: 11320098]
22. Chakraborty S, John R, Nag A. Cytoglobin in tumor hypoxia: novel insights into cancer suppression. Tumour Biol 2014 7;35(7):6207–19. [PubMed: 24816917]
23. Liu X, El-Mahdy MA, Boslett J, Varadharaj S, Hemann C, Abdelghany TM, Ismail RS, Little SC, Zhou D, Thuy LT, Kawada N, Zweier JL. Cytoglobin regulates blood pressure and vascular tone through nitric oxide metabolism in the vascular wall. Nat Commun 2017 4 10;8:14807.
24. Sugimoto H, Makino M, Sawai H, Kawada N, Yoshizato K, Shiro Y. Structural basis of human cytoglobin for ligand binding. J Mol Biol 2004 6 11;339(4):873–85. [PubMed: 15165856]
25. Thuy le TT, Morita T, Yoshida K, Wakasa K, Iizuka M, Ogawa T, Mori M, Sekiya Y, Momen S, Motoyama H, Ikeda K, Yoshizato K, Kawada N. Promotion of liver and lung tumorigenesis in DEN-treated cytoglobin-deficient mice. Am J Pathol 2011 8;179(2):1050–60. [PubMed: 21684245]
26. Thuy le TT, Matsumoto Y, Thuy TT, Hai H, Suoh M, Urahara Y, Motoyama H, Fujii H, Tamori A, Kubo S, Takemura S, Morita T, Yoshizato K, Kawada N. Cytoglobin deficiency promotes liver cancer development from hepatosteatosis through activation of the oxidative stress pathway. Am J Pathol 2015 4;185(4):1045–60. [PubMed: 25665792]
27. Thuy le TT, Van Thuy TT, Matsumoto Y, Hai H, Ikura Y, Yoshizato K, Kawada N. Absence of cytoglobin promotes multiple organ abnormalities in aged mice. Sci Rep 2016 5 5;6:24990. [PubMed: 27146058]
28. Schmidt M, Laufs T, Reuss S, Hankeln T, Burmester T. Divergent distribution of cytoglobin and neuroglobin in the murine eye. Neurosci Lett 2005 2 21;374(3):207–11. [PubMed: 15663964]
29. Ostojić J, Sakaguchi DS, de Lathouder Y, Hargrove MS, Trent JT 3rd, Kwon YH, Kardon RH, Kuehn MH, Betts DM, Grozdanić S. Neuroglobin and cytoglobin: oxygen-binding proteins in retinal neurons. Invest Ophthalmol Vis Sci 2006 3;47(3):1016–23. [PubMed: 16505036]
30. Reuss S, Wystub S, Disque-Kaiser U, Hankeln T, Burmester T. Distribution of Cytoglobin in the Mouse Brain. Front Neuroanat 2016 4 27;10:47. [PubMed: 27199679]
31. Alves CH, Sanz AS, Park B, Pellissier LP, Tanimoto N, Beck SC, Huber G, Murtaza M, Richard F, Sridevi Gurubaran I, Garcia Garrido M, Levelt CN, Rashbass P, Le Bivic A, Seeliger MW, Wijnholds J. Loss of CRB2 in the mouse retina mimics human retinitis pigmentosa due to mutations in the CRB1gene. Hum Mol Genet 2013 1 1;22(1):35–50. [PubMed: 23001562]
32. Pellissier LP, Alves CH, Quinn PM, Vos RM, Tanimoto N, Lundvig DM, Dudok JJ, Hooibrink B, Richard F, Beck SC, Huber G, Sothilingam V, Garcia Garrido M, Le Bivic A, Seeliger MW, Wijnholds J. Targeted ablation of CRB1 and CRB2 in retinal progenitor cells mimics Leber congenital amaurosis. PLoS Genet 2013;9(12):e1003976. [PubMed: 24339791]
33. van Rossum AG, Aartsen WM, Meuleman J, Klooster J, Malysheva A, Versteeg I, Arsanto JP, Le Bivic A, Wijnholds J. Pals1/Mpp5 is required for correct localization of Crb1 at the subapical region in polarized Muller glia cells. Hum Mol Genet 2006 9 15;15(18):2659–72 [PubMed: 16885194]
34. Dudok JJ, Sanz AS, Lundvig DM, Wijnholds J. MPP3 is required for maintenance of the apical junctional complex, neuronal migration, and stratification in the developing cortex. J Neurosci 2013 5 8;33(19):8518–27. [PubMed: 23658188]
35. Dudok JJ, Sanz AS, Lundvig DM, Sothilingam V, Garcia Garrido M, Klooster J, Seeliger MW, Wijnholds J. MPP3 regulates levels of PALS1 and adhesion between photoreceptors and Müller cells. Glia 2013 10;61(10):1629–44. [PubMed: 23893895]
36. Park B, Alves CH, Lundvig DM, Tanimoto N, Beck SC, Huber G, Richard F, Klooster J, Andlauer TF, Swindell EC, Jamrich M, Le Bivic A, Seeliger MW, Wijnholds J. PALS1 is essential for retinal pigment epithelium structure and neural retina stratification. J Neurosci 2011 11 23;31(47):17230–41. [PubMed: 22114289]
37. Kim S, Lehtinen MK, Sessa A, Zappaterra MW, Cho SH, Gonzalez D, Boggan B, Austin CA, Wijnholds J, Gambello MJ, Malicki J, LaMantia AS, Broccoli V, Walsh CA. The apical complex

couples cell fate and cell survival to cerebral cortical development. Neuron 2010 4 15;66(1):69–84. [PubMed: 20399730]

38. Cho SH, Kim JY, Simons DL, Song JY, Le JH, Swindell EC, Jamrich M, Wu SM, Kim S. Genetic ablation of Pals1 in retinal progenitor cells models the retinal pathology of Leber congenital amaurosis. Hum Mol Genet 2012 6 15;21(12):2663–76. [PubMed: 22398208]
39. Koike C, Nishida A, Akimoto K, Nakaya MA, Noda T, Ohno S, Furukawa T. Function of atypical protein kinase C lambda in differentiating photoreceptors is required for proper lamination of mouse retina. J Neurosci 2005 11 2;25(44):10290–8. [PubMed: 16267237]
40. Heynen SR, Meneau I, Caprara C, Samardzija M, Imsand C, Levine EM, Grimm C. CDC42 is required for tissue lamination and cell survival in the mouse retina. PLoS One 2013;8(1):e53806. [PubMed: 23372671]
41. Sottocornola R, Royer C, Vives V, Tordella L, Zhong S, Wang Y, Ratnayaka I, Shipman M, Cheung A, Gaston-Massuet C, Ferretti P, Molnár Z, Lu X. ASPP2 binds Par-3 and controls the polarity and proliferation of neural progenitors during CNS development. Dev Cell 2010 7 20;19(1):126–37. [PubMed: 20619750]
42. Ali M, Hocking PM, McKibbin M, Finnegan S, Shires M, Poulter JA, Prescott K, Booth A, Raashid Y, Jafri H, Ruddle JB, Mackey DA, Jacobson SG, Toomes C, Lester DH, Burt DW, Curry WJ, Inglehearn CF. Mpdz null allele in an avian model of retinal degeneration and mutations in human leber congenital amaurosis and retinitis pigmentosa. Invest Ophthalmol Vis Sci 2011 9 27;52(10):7432–40. [PubMed: 21862650]
43. Moore BA, Leonard BC, Sebbag L, Edwards SG, Cooper A, Imai DM, Straiton E, Santos L, Reilly C, Griffey SM, Bower L, Clary D, Lloyd KCK, Murphy CJ, Moshiri A. Identification of genes required for eye development by high-throughput screening of mouse knockouts. Communications Biology doi: 10.1038/s42003-018-0226-0
44. Yzer S, Fishman GA, Racine J, Al-Zuhaibi S, Chakor H, Dorfman A, Szlyk J, Lachapelle P, van den Born LI, Allikmets R, Lopez I, Cremers FP, Koenekoop RK. CRB1 heterozygotes with regional retinal dysfunction: implications for genetic testing of leber congenital amaurosis. Invest Ophthalmol Vis Sci 2006 9;47(9):3736–44. [PubMed: 16936081]
45. Zernant J, Külm M, Dharmaraj S, den Hollander AI, Perrault I, Preising MN, Lorenz B, Kaplan J, Cremers FP, Maumenee I, Koenekoop RK, Allikmets R. Genotyping microarray (disease chip) for Leber congenital amaurosis: detection of modifier alleles. Invest Ophthalmol Vis Sci 2005 9;46(9): 3052–9. [PubMed: 16123401]
46. van den Hurk JA, Rashbass P, Roepman R, Davis J, Voesenek KE, Arends ML, Zonneveld MN, van Roekel MH, Cameron K, Rohrschneider K, Heckenlively JR, Koenekoop RK, Hoyng CB, Cremers FP, den Hollander AI. Characterization of the Crumbs homolog 2 (CRB2) gene and analysis of its role in retinitis pigmentosa and Leber congenital amaurosis. Mol Vis 2005 4 15;11:263–73. [PubMed: 15851977]
47. Xiao Z, Patrakka J, Nukui M, Chi L, Niu D, Betsholtz C, Pikkarainen T, Vainio S, Tryggvason K. Deficiency in Crumbs homolog 2 (Crb2) affects gastrulation and results in embryonic lethality in mice. Dev Dyn 2011 12;240(12):2646–56. [PubMed: 22072575]
48. Geuens E, Brouns I, Flamez D, Dewilde S, Timmermans JP, Moens L A globin in the nucleus! J. Biol. Chem, 278 (2003), pp. 30417–30420 [PubMed: 12796507]
49. Schmidt M, Gerlach F, Avivi A, Laufs T, Wystub S, Simpson JC, Nevo E, Saaler-Reinhardt S, Reuss S, Hankeln T, Burmester T Cytoglobin is a respiratory protein in connective tissue and neurons, which is up-regulated by hypoxia. J. Biol. Chem, 279 (2004), pp. 8063–8069 [PubMed: 14660570]
50. Moore BA, Leonard BC, Sebbag L, Edwards SG, Cooper A, Imai DM, Straiton E, Santos L, Reilly C, Griffey SM, Bower L, Clary D, Mason J, Roux MJ, Meziane H, Herault Y; International Mouse Phenotyping Consortium, McKerlie C, Flenniken AM, Nutter LMJ, Berberovic Z, Owen C, Newbigging S, Adissu H, Eskandarian M, Hsu CW, Kalaga S, Udensi U, Asomugha C, Bohat R, Gallegos JJ, Seavitt JR, Heaney JD, Beaudet AL, Dickinson ME, Justice MJ, Philip V, Kumar V, Svenson KL, Braun RE, Wells S, Cater H, Stewart M, Clementson-Mobbs S, Joynson R, Gao X, Suzuki T, Wakana S, Smedley D, Seong JK, Tocchini-Valentini G, Moore M, Fletcher C, Karp N, Ramirez-Solis R, White JK, de Angelis MH, Wurst W, Thomasy SM, Flicek P, Parkinson H, Brown SDM, Meehan TF, Nishina PM, Murray SA, Krebs MP, Mallon AM, Lloyd KCK, Murphy

CJ, Moshiri A. Identification of genes required for eye development by high-throughput screening of mouse knockouts.Commun Biol 2018 12 21;1:236. [PubMed: 30588515]

51. Hundahl CA, Allen GC, Hannibal J, Kjaer K, Rehfeld JF, Dewilde S, Nyengaard JR, Kelsen J, Hay-Schmidt A. Anatomical characterization of cytoglobin and neuroglobin mRNA and protein expression in the mouse brain. Brain Res 2010 5 17;1331:58–73. [PubMed: 20331985]
52. Fago A, Hundahl C, Dewilde S, Gilany K, Moens L, Weber RE. Allosteric regulation and temperature dependence of oxygen binding in human neuroglobin and cytoglobin. Molecular mechanisms and physiological significance. J Biol Chem 2004 10 22;279(43):44417–26. [PubMed: 15299006]
53. Gabba M, Abbruzzetti S, Spyrakis F, Forti F, Bruno S, Mozzarelli A, Luque FJ, Viappiani C, Cozzini P, Nardini M, Germani F, Bolognesi M, Moens L, Dewilde S. CO rebinding kinetics and molecular dynamics simulations highlight dynamic regulation of internal cavities in human cytoglobin. PLoS One 2013;8(1):e49770. [PubMed: 23308092]
54. Gardner AM, Cook MR, Gardner PR. Nitric-oxide dioxygenase function of human cytoglobin with cellular reductants and in rat hepatocytes. J Biol Chem 2010 285(31):23850–23857. [PubMed: 20511233]
55. Gardner PR. Nitric oxide dioxygenase function and mechanism of flavohemoglobin, hemoglobin, myoglobin and their associated reductases. J Inorg Biochem 2005 99(1):247–266. [PubMed: 15598505]
56. Vinogradov SN, Moens L. Diversity of globin function: enzymatic, transport, storage, and sensing. J Biol Chem 2008 283(14):8773–8777. [PubMed: 18211906]
57. Gardner PR, Gardner AM, Brashear WT, Suzuki T, Hvitved AN, Setchell KD, Olson JS. Hemoglobins dioxygenate nitric oxide with high fidelity. J Inorg Biochem 2006 100(4):542–550. [PubMed: 16439024]
58. Kawada N, Kristensen DB, Asahina K, Nakatani K, Minamiyama Y, Seki S, Yoshizato K. Characterization of a stellate cell activation-associated protein (STAP) with peroxidase activity found in rat hepatic stellate cells. J Biol Chem 2001 276(27):25318–25323 [PubMed: 11320098]
59. Trent JT, Hargrove MS. A ubiquitously expressed human hexacoordinate hemoglobin. J Bio Chem 2002 277(22):19538–19545 [PubMed: 11893755]
60. Fordel E, Thijs L, Martinet W, Schrijvers D, Moens L, Dewilde S. Anoxia or oxygen and glucose deprivation in SH-SY5Y cells: a step closer to the unraveling of neuroglobin and cytoglobin functions. Gene 2007 398(1–2):114–122 [PubMed: 17532579]
61. Hodges NJ, Innocent N, Dhanda S, Graham M. Cellular protection from oxidative DNA damage by over-expression of the novel globin cytoglobin in vitro. Mutagenesis 2008 23(4):293–298. [PubMed: 18353768]
62. Bujakowska K, Audo I, Mohand-Saïd S, Lancelot ME, Antonio A, Germain A, Léveillard T, Letexier M, Saraiva JP, Lonjou C, Carpentier W, Sahel JA, Bhattacharya SS, Zeitz C. CRB1 mutations in inherited retinal dystrophies. Hum Mutat 2012 2;33(2):306–15. [PubMed: 22065545]
63. Moshiri A, Humpal D, Leonard BC, Imai DM, Tham A, Bower L, Clary D, Glaser TM, Lloyd KC, Murphy CJ. Arap1 Deficiency Causes Photoreceptor Degeneration in Mice. Invest Ophthalmol Vis Sci 2017 3 1;58(3):1709–1718. [PubMed: 28324111]
64. Sun N, Shibata B, Hess JF, FitzGerald PG. An alternative means of retaining ocular structure and improving immunoreactivity for light microscopy studies. Mol Vis 2015 4 16;21:428–42. [PubMed: 25991907]
65. Sanes JR, Rubenstein JL, Nicolas JF. Use of a recombinant retrovirus to study post-implantation cell lineage in mouse embryos. EMBO J 1986 12 1;5(12):3133–42. [PubMed: 3102226]

Highlights

- Cytoglobin is expressed in mature inner retinal neurons (retinal ganglion cells and amacrine cells)
- Cytoglobin deficiency potentiates cell polarity defects in Crb1-deficient rd8 retina
- Cytoglobin deficiency results in cell polarity gene alterations
- Cytoglobin may explain in part the diversity of CRB1 related retinopathies seen in patients as a modulator of this pathway

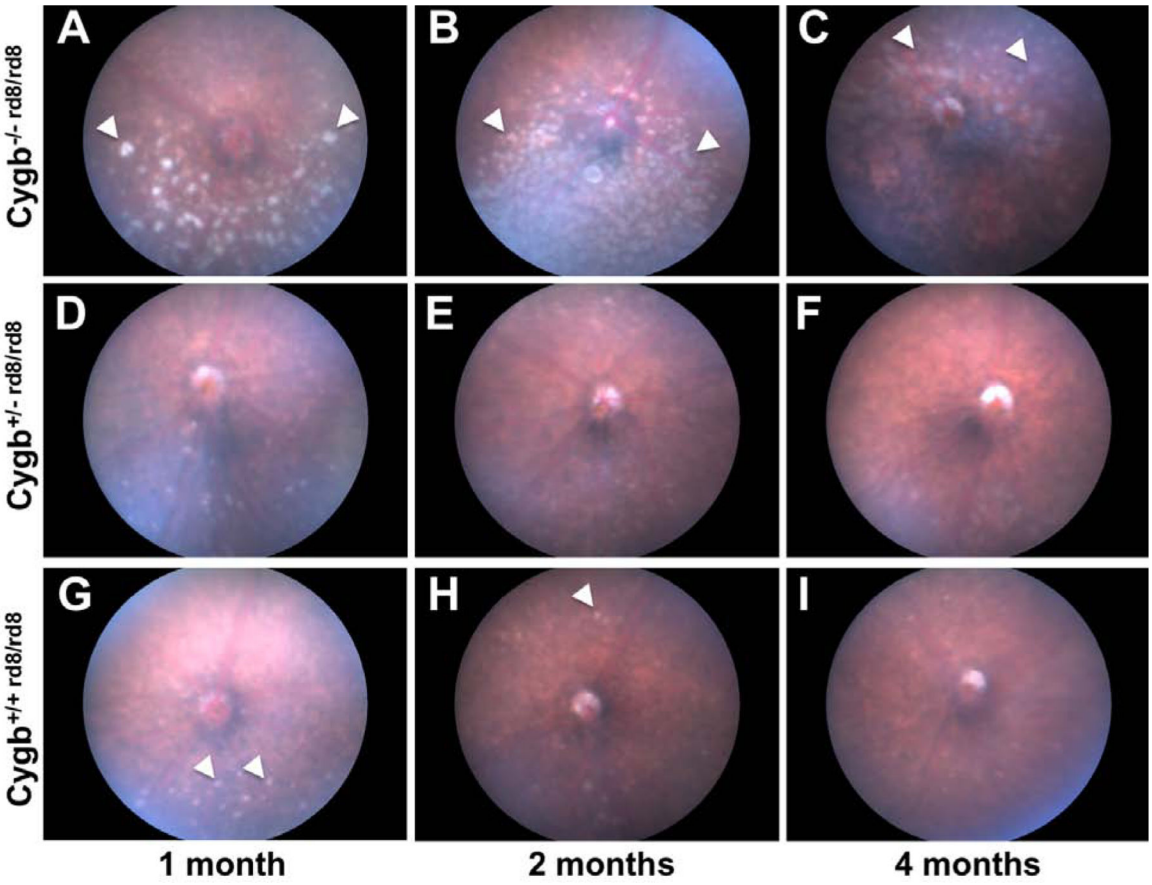

Figure 1:

Cytoglobin deficiency potentiates the severity of the rd8 fundus phenotype. $Cygb^{-/-rd8/rd8}$ mice (A, B, C) accumulate an increased number and size of fundus flecks (arrowheads) when compared to $Cygb^{+/+rd8/rd8}$ mice (G, H, I) at all ages examined. By 2 months of age, the inferior fundus of $Cygb^{-/-rd8/rd8}$ animals develops confluent flecks (B), which undergo pigmentary atrophy (C) by 4 months. The number and size of flecks in $Cygb^{+/-rd8/rd8}$ mice (D, E, F) is indistinguishable from $Cygb^{+/+rd8/rd8}$ littermates (G, H, I) at all ages examined. See quantification of white spots in Supplemental Figure 1. For each genotype $n > 15$.

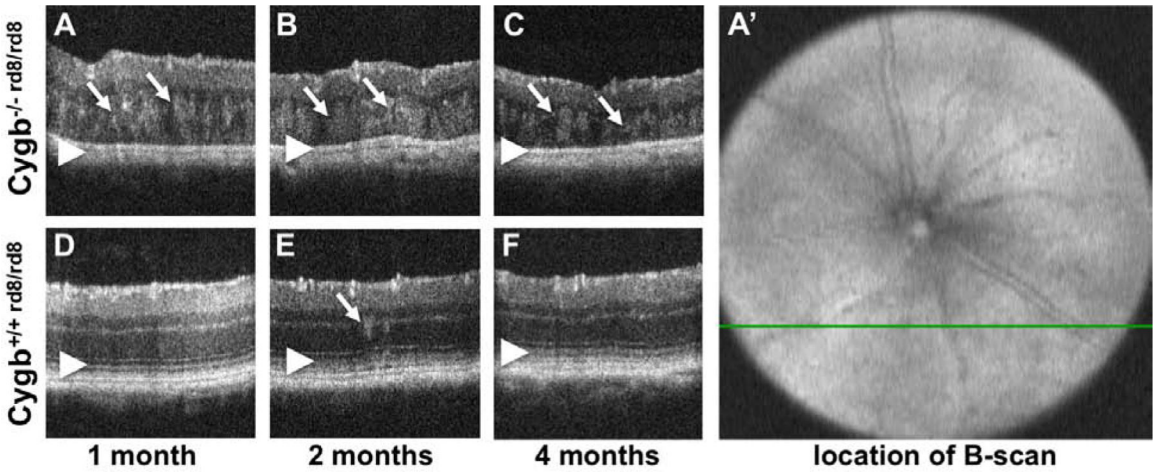

Figure 2:

Optical Coherence Tomography of Cygb$^{-/-rd8/rd8}$ mice shows outer retinal hyperreflective foci and loss of outer retinal bands. Areas of hyperreflectivity are seen as early as post-natal month 1 (A, arrows), and persist at postnatal month 2 (B, arrows) and 4 (C, arrows). Similar lesions are occasionally see in Cygb$^{+/+rd8/rd8}$ animals (D,E,F) at these ages (arrow in E), but to a lesser degree. The outer retinal bands (D,E,F, arrowheads) representing the external limiting membrane, the inner segment/outer segment junction (aka ellipsoid zone), and the retinal pigmented epithelium are not discernable in Cygb$^{-/-rd8/rd8}$ mice (A,B,C arrowheads). Also, the total thickness of the retina decreases with age in Cygb$^{-/-rd8/rd8}$ mice (A,B,C). The b-scans shown here are taken from horizontal scans in the inferior retina. For example, the green line in A' corresponds to the cross section in panel A.

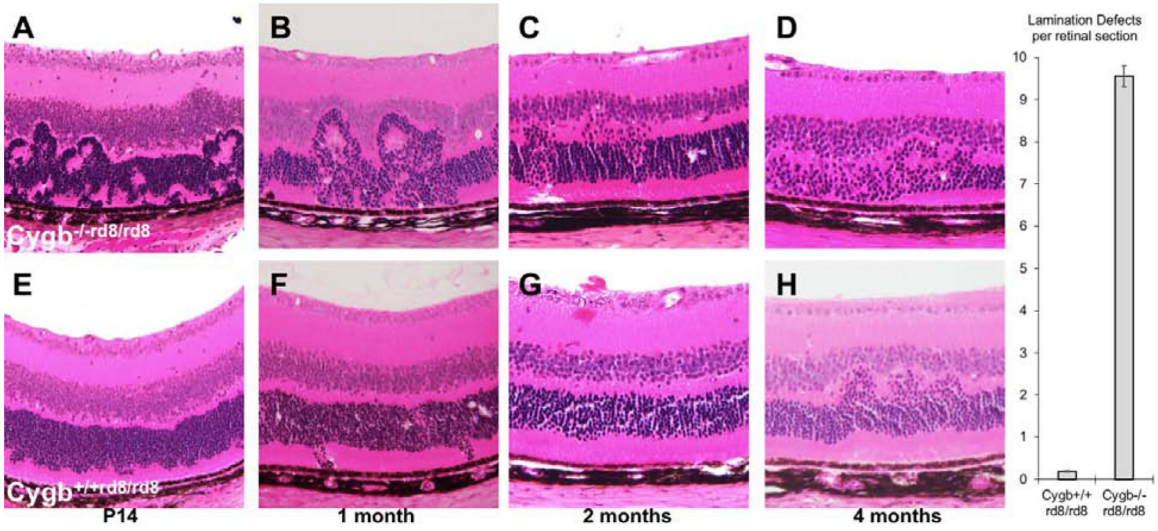

Figure 3:

Cygb deficiency increases the severity of photoreceptor lamination defects in rd8 mice. At several postnatal ages, hematoxylin and eosin histological analysis of the outer nuclear layer in Cygb$^{-/-rd8/rd8}$ retina on the rd8 background (A-C) has profound outer retinal lamination defects with photoreceptor rosettes that eventually lead to photoreceptor loss (D). Cygb $^{+/+rd8/rd8}$ mice (E-H) have less severe lamination defects that progress less rapidly and without obvious cell loss at these time points. (n = 5 each group).

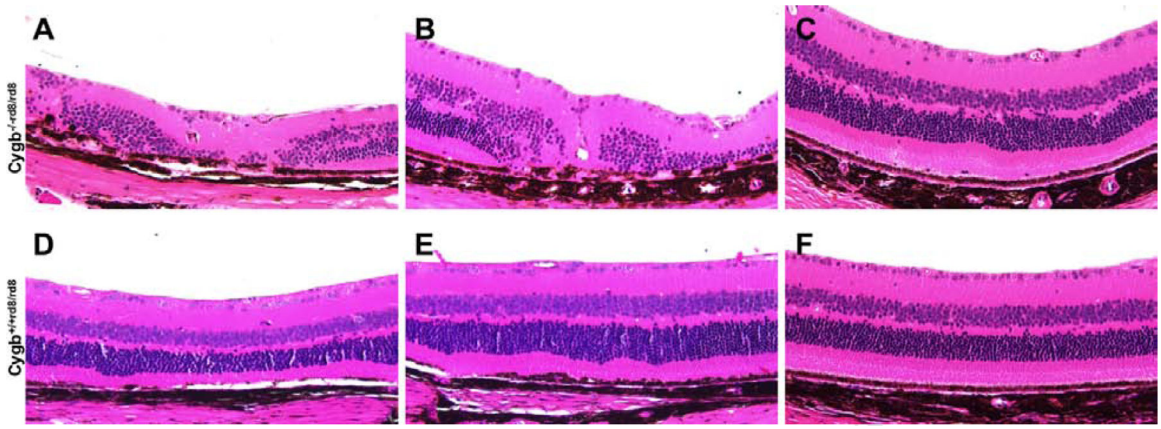

Figure 4:

Cygb deficiency leads to severe retinal degeneration in aged rd8 mice. At 24 months postnatal age, $Cygb^{-/-rd8/rd8}$ mice on the rd8 background (A-C) have areas of mild, moderate, and severe retinal degeneration within the same eye. $Cygb^{+/+rd8/rd8}$ mice (D-F) have areas of normal to mild retinal degeneration at this stage. (n = 6 each group).

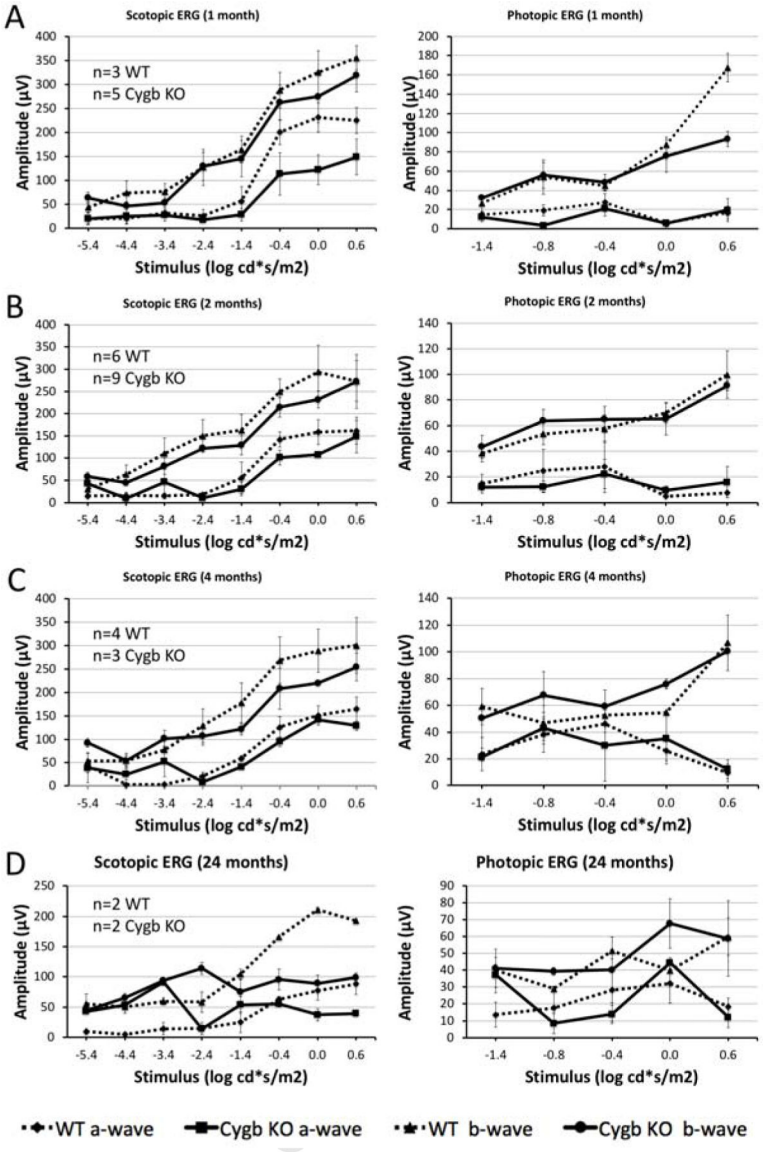

Figure 5:

Rod retinal function declines with age in Cygb deficient rd8 mice. Scotopic (dark-adapted) and photopic (light-adapted) electroretinography was performed in Cygb$^{-/-rd8/rd8}$ (designated Cygb KO) mice and Cygb$^{+/+rd8/rd8}$ (designated WT) controls at one (A), 2 (B), 4 (C), and 24 (D) months postnatal age. Stimulus-response curves are shown with absolute values of the a- and b-waves for Cygb$^{-/-rd8/rd8}$ (solid line) and Cygb$^{+/+rd8/rd8}$ (dashed line) on the same graphs. At 1- and 2-months postnatal age, rod and cone mediated retinal pathways appear similar in both groups. By 4 months of age (C) the scotopic b-wave declines in Cygb$^{-/-rd8/rd8}$ mice when compared to Cygb$^{+/+rd8/rd8}$ mice at this age. By 24 months postnatal age, the scotopic b-wave is markedly reduced in comparison to Cygb $^{+/+rd8/rd8}$ mice. Photopic responses appear similar at all stages in both groups, suggesting less involvement of the cone-mediated responses. (Exact n is shown in figure for each time point. For A-C, n≥3 in each group. n=2 in each group for panel D).

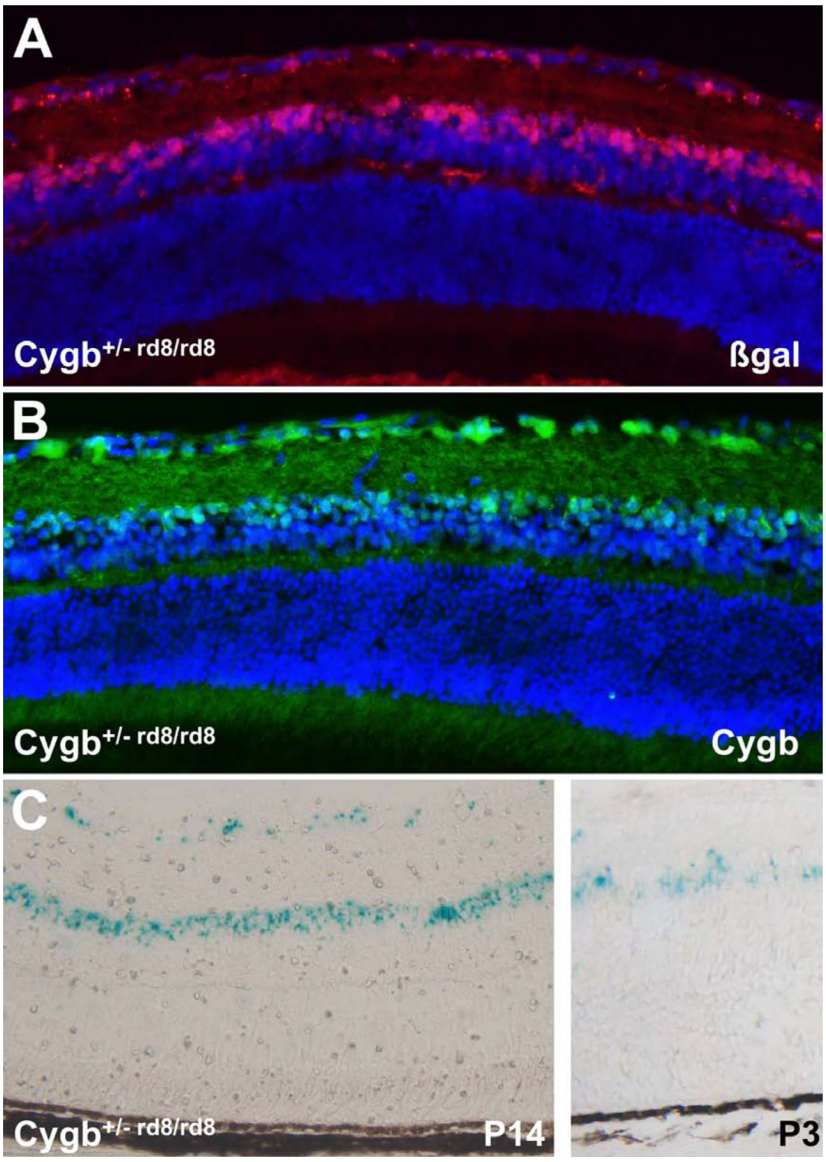

Figure 6:

Cygb is expressed in the inner retina. Immunohistochemistry at postnatal age 1 month using anti-ß-galactosidase antibodies as a surrogate for Cygb expression (A) shows expression in the retinal ganglion cell layer and the inner aspect of the inner nuclear layer. Anti-Cygb staining (B) is seen in a similar pattern as anti-ß-galactosidase at the same age. LacZ histochemistry corroborates this expression pattern in postnatal day 14 heterozygous mice (C, left), and in neonatal heterozygous mice at postnatal day 3 (C, right).

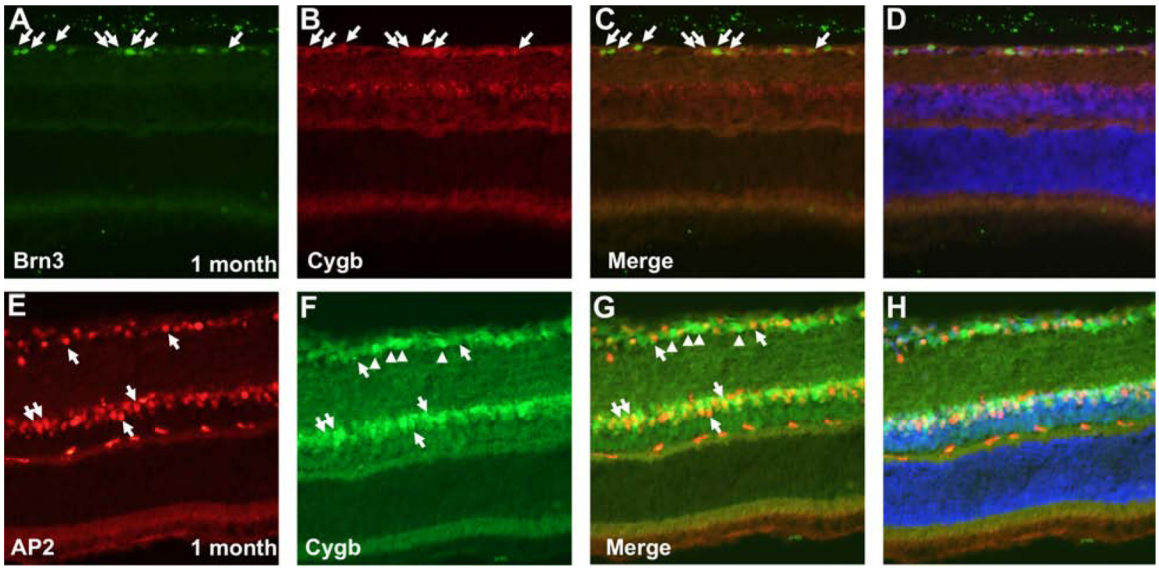

Figure 7:

Cygb is expressed in retinal ganglion cells and amacrine cells. Double-labeling at postnatal age 1 month using (A-D) anti-Cygb and anti-Brn3, or (E-H) anti-Cygb and anti-AP2 show co-labeling in both retinal ganglion cells and amacrine neurons, respectively. Cytoglobin is localized both to the cytoplasmic and nuclear compartments in these neurons. Arrows point to cells expressing both markers. Arrowheads in E-H point to cells in the ganglion cell layer that are Cygb-positive but AP2-negative, and likely represent RGCs.

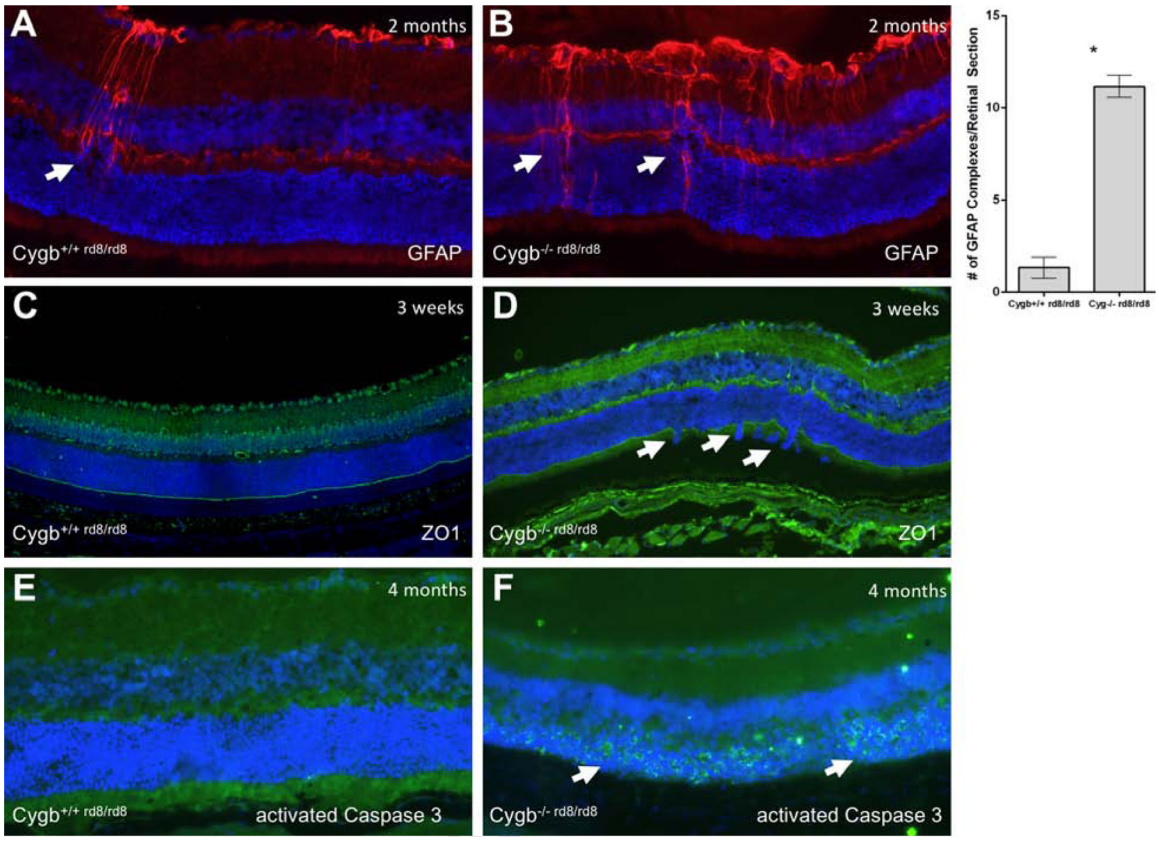

Figure 8:

Cygb deficiency results in disruption of the outer limiting membrane, reactive Muller glia, and cell death. Typical anti-GFAP staining is show in (A) Cygb$^{+/+rd8/rd8}$ mice and (B) Cygb $^{-/-rd8/rd8}$ mice at postnatal age 2 months. Quantification of GFAP-positive activated Muller glial complexes per retinal section is shown (*P<0.05 was considered significant, student's t-test). The outer limiting membrane as stained by anti-ZO1 immunohistochemistry show relative preservation of this structure in (A) Cygb$^{+/+rd8/rd8}$ mice, but with frequent areas of discontinuity seen in (B) Cygb$^{-/-rd8/rd8}$ mice at postnatal age 3 weeks. Virtually no anti-activated Caspase 3 staining is seen at postnatal age 4 months in (E) the Cygb$^{+/+rd8/rd8}$ retina, while robust staining is seen in the outer nuclear layer at this age in (F) Cygb$^{-/-rd8/rd8}$ mice.

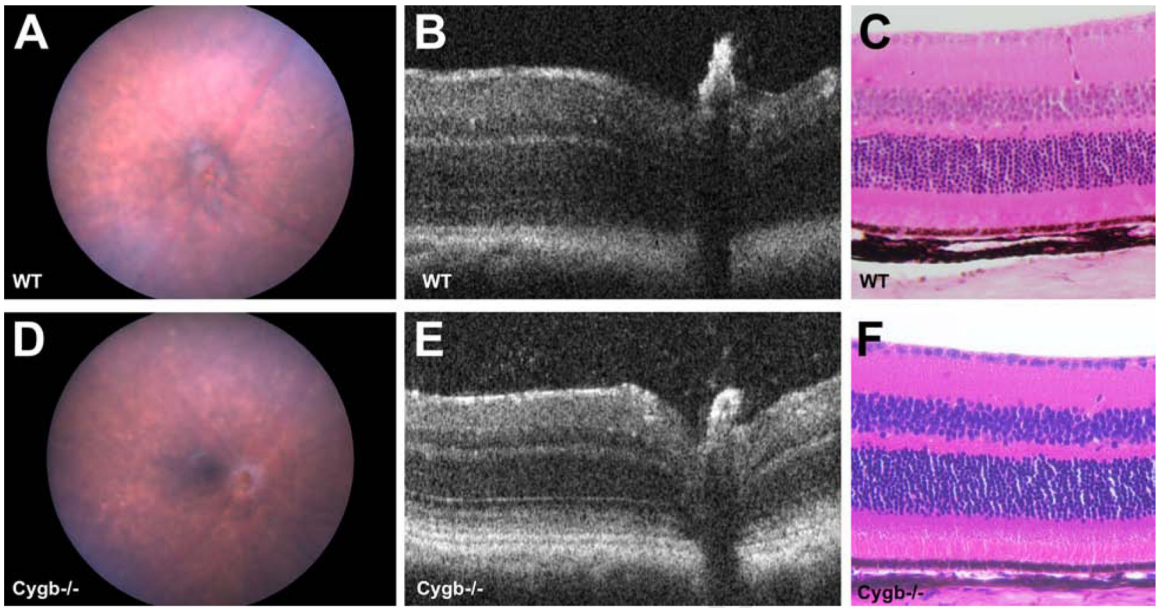

Figure 9:

Cygb knockout mice free from the rd8 mutation have no obvious retinal abnormalities. Color fundus photos of (A) WT and (B) Cygb$^{-/-}$ mice on the C57BL/6J background confirmed to be free of the rd8 mutation are indistinguishable at 4 months postnatal age. Spectral domain optical coherence tomography (SD-OCT) of (C) WT and (D) Cygb$^{-/-}$ mice show similar retinal lamination, which is consistent with (E,F) the hematoxylin and eosin histological analysis at 4 months postnatal.

Table 1:

Cygb$^{-/-}$ retinas have modest transcriptional dysregulation of genes related to cell polarity, oxidative stress, and nitric oxide signaling.

Quantitative PCR from cDNAs derived from Cygb$^{-/-}$ and wild type retinas were compared, while Cygb$^{-/-\ rd8/rd8}$ retinas were compared with Cygb$^{+/+\ rd8/rd8}$ controls. Retinas from animals at age 1 month were used. Twelve (bold) of 17 cell polarity related genes tested were altered at the transcriptional level in the Cygb$^{-/-}$ retina compared to WT controls free of the rd8 mutation. However, no transcriptional alterations were detected between Cygb$^{-/-\ rd8/rd8}$ when compared to Cygb$^{+/+\ rd8/rd8}$ controls. Modest alterations in genes related to NO-signaling were seen in Cygb$^{-/-}$ retinas but not in Cygb$^{-/-\ rd8/rd8}$ counterparts. Genes related to oxidative stress were altered in both Cygb$^{-/-}$ and Cygb$^{-/-rd8/rd8}$ animals. Relative expression levels are reported as RQ value (fold change) for each gene using the ΔΔC(t) method. (*P*-value <0.05 was considered significant; n=3 biological replicates for each genotype, and n=3 technical replicates for each gene).

	Cygb−/−		**Cygb−/− rd8/rd8**	
Gene	**RQ**	***P*-value**	**RQ**	***P*-value**
Cell polarity				
Crb1	1.136	0.130	1.036	0.340
Crb2	**0.738**	**0.020**	0.976	0.440
Cdc42	**0.687**	**0.0005**	0.984	0.690
Prkci	**0.791**	**0.020**	1.087	0.460
Prkcz	**0.815**	**0.020**	1.109	0.470
Pard6a	**0.765**	**0.040**	1.109	0.120
Pard6b	**0.795**	**0.010**	1.121	0.490
Pard6g	**0.730**	**0.020**	1.017	0.960
Pard3	**0.814**	**0.010**	1.121	0.550
Tiam1	0.792	0.110	0.988	0.950
TIam2	2.644	0.170	0.555	0.053
RacGap1	**0.684**	**0.002**	1.099	0.230
MPP5	**0.674**	**0.0003**	1.084	0.580
Lin7a	**0.627**	**0.0002**	0.766	0.110
MPDZ	**0.791**	**0.01**	1.136	0.620
Patj	1.161	0.610	0.743	0.210
Tjp1	1.204	0.290	1.022	0.890
Oxidative Stress				
Aass	0.737	0.068	**0.761**	**0.046**
Gpx1	**0.717**	**0.00001**	1.007	0.977
NO signaling				
Hpn	**0.521**	**0.013**	0.628	0.212
Pea15a	**0.670**	**0.002**	1.058	0.563
Rprm	1.280	0.597	0.745	0.220

Table 2:

Primer sequences used for quantitative PCR experiments.

GENE	SEQUENCES
Crb1 Forward	TTGGTCAACAGGTTCCTATGC
Crb1 Reverse	AGCCTGTCATCAGCCAGGT
Crb2 Forward	CCCCTTAGGCACCAACTG
Crb2 Reverse	TTCACAGGGTTTGTCGAGACT
Cdc42 Forward	CCCATCGGAATATGTACCAACTG
Cdc42 Reverse	CCAAGAGTGTATGGCTCTCCAC
Prkci Forward	TGACTACGGCATGTGTAAGGA
Prkci Reverse	CCGCAGAAAGTGCTGGTT
Prkcz Forward	GGGACGAAGTGCTCATCATT
Prkcz Reverse	CACGGCGGTAGATGGACT
Pard6a Forward	CCCTCACCAACGATGACAGT
Pard6a Reverse	GCCACTCGAGTCACCTTCC
Pard6b Forward	GGGCACTCAGCATGAACC
Pard6b Reverse	CGACGAAACTCAGCTCCAA
Pard6g Forward	CATAAGTCTCAGACCCTACGCT
Pard6g Reverse	GGTCACCTCGGTGTTAGAGATG
Pard3 Forward	TTGTATGCCCAAGTAAAGAAACC
Pard3 Reverse	TCATGGTTGCTAGGAGTGGA
Tiam1 Forward	GGAATATTTGATGACACTGTTCCA
Tiam1 Reverse	GGTGGACACTGGGTAAGACC
Tiam2 Forward	ACATGGTTGGACTCATGGGAG
Tiam2 Reverse	TGGTGCCCTTTGAGACTTTACA
RacGap1 Forward	GACCTTCTGGCTGAGCAAA
RacGap1 Reverse	CGGCTGTGCTGTTGTCTTC
MPP5 Forward	TGATTCCTAGTCAACAGATCAAGC
MPP5 Reverse	GGGTCATCTGAGGGGTCATA
Lin7a Forward	TCTCGTGTGTACACTGTAAGAGAATTT
Lin7a Reverse	CTTCGCTGGCTGCAAAAG
MPDZ Forward	AGGAGATTCAGGAGGGCAGT
MPDZ Reverse	AGGATCTGGTCGGTTTCCTTA
Patj Forward	TCTACTTGGAGTCCTAACAGGC
Patj Reverse	GGCATACTTGCTGAGCAGTGT
Tjp1 Forward	ATGCAGACCCAGCAAAGG
Tjp1 Reverse	GGGTGACCAAGAGCTGGTT
Aass Forward	GGCATCACCAAACTGGGCTA
Aass Reverse	CAACAGGTTCATATTGGCTTCCT
Gpx1 Forward	AGTCCACCGTGTATGCCTTCT

GENE	SEQUENCES
Gpx1 Reverse	GAGACGCGACATTCTCAATGA
Hpn Forward	TGGGCCATTGTGACCATCCTA
Hpn Reverse	TCCGTCTTGTCCAACACTGC
Pea15a Forward	GCCTGGTTCATCTCCCAGTA
Pea15a Reverse	TGCTCAATGTAGGAGAGGTTGTC
Rprm Forward	AGCAGGTGGCAAAAGCAG
Rprm Reverse	GCCTGGTTCATCTCCCAGTA
Rhodopsin Forward	CCCTTCTCCAACGTCACAGG
Rhodopsin Reverse	TGAGGAAGTTGATGGGGAAGC